

Electron-energy-loss study of the $\text{TiO}_2(110)$ surface

Mohamed H. Mohamed,* Hassan R. Sadeghi,[†] and Victor E. Henrich
Applied Physics Department, Yale University, New Haven, Connecticut 06520

(Received 6 July 1987)

Electron-energy-loss measurements on the stoichiometric $\text{TiO}_2(110)$ surface which include electronic excitations from both the O $2p$ valence states and the O $2s$, Ti $3p$, and Ti $3s$ core levels have been performed. The observed features have been empirically interpreted within the framework of the molecular-orbital description of an octahedral complex. The effects of surface defects created by Ar^+ -ion bombardment and by the evaporation of a thin Ti overlayer on the energy-loss results have also been studied and were found to cause marked changes in both the valence and core loss spectra. This sensitivity arises from changes in the screening between surface cations that occur when the oxygen-titanium ratio at the surface is varied.

I. INTRODUCTION

During the past decade there has been an increasing interest in the study of the electronic properties of transition-metal oxide surfaces, particularly TiO_2 . The discovery of its photocatalytic potential¹ and later its role in the strong metal-support interaction^{2,3} (SMSI) spurred a sustained interest in the study of the electronic properties of both nearly perfect and defect-containing surfaces as well as in understanding the interaction of such surfaces with adsorbed molecules. For this purpose, a variety of surface-spectroscopic techniques have been utilized, the results of which have been discussed in recent reviews.⁴⁻⁶

Although several reflection electron-energy-loss (EELS) studies of the $\text{TiO}_2(110)$ surface have been reported, most of them have dealt only with the electronic transitions originating from the O $2p$ valence states.⁷⁻⁹ However, excitations involving the core levels are also of interest, particularly in view of the recent correlation between the desorption of positive ions, such as O^+ , and the onset of the Ti $3p$ core-level excitations of TiO_2 .^{10,11} A number of reflection EELS measurements involving excitation of the Ti $3p$ core level have been previously reported for TiO_2 (Ref. 10) and for polycrystalline titanium exposed to oxygen.^{12,13} However, the results obtained for oxidized titanium neither agreed with each other nor with those obtained for TiO_2 . There is thus a need for complete EELS spectra encompassing both the transitions originating from the O $2p$ valence states and those originating from the shallow core levels (O $2s$, Ti $3p$, and Ti $3s$) of well-characterized TiO_2 surfaces. We have chosen the (110) surface of TiO_2 since it is known to be the most stable surface and has been rather thoroughly studied by other surface science techniques.⁴ In addition, we have investigated the effect of surface defects and a Ti overlayer on the excitations of the $\text{TiO}_2(110)$ surface.

II. EXPERIMENT

The $\text{TiO}_2(110)$ surface was prepared in ultrahigh vacuum [$(2-4) \times 10^{-10}$ Torr] by bombarding a single-crystal

sample with 500-eV Ar^+ ions followed by annealing for 10–15 min at 673 K in 10^{-6} Torr O_2 . The sample was then allowed to cool to room temperature in the ambient O_2 . Such a treatment resulted in an atomically clean surface exhibiting (1×1) LEED patterns and having a surface defect density below the detection capabilities of both ultraviolet photoemission spectroscopy (UPS) and EELS. Defect surface states on TiO_2 are manifested by a loss peak at about 1.5–2 eV in EELS spectra and by emission in the bulk-band-gap region in UPS spectra.¹⁴ Energy-loss spectra were obtained by using a double-pass cylindrical-mirror analyzer (CMA) having a coaxial electron gun. Primary electrons were incident perpendicular to the sample surface.

The spectra were recorded as the first derivative of the secondary-electron distribution versus loss energy, $dn(E)/dE$, by applying a 0.5-V peak-to-peak modulating voltage to the incident electron-beam energy followed by phase-sensitive detection of the reflected electrons. The locations of peaks in $n(E)$ correspond to maximum negative slopes in the resulting EELS spectra; the energies of all of our loss features are taken at the point of maximum negative slope. The overall system resolution, as measured by the full width at half maximum (FWHM) of the elastic peaks, was maintained at 0.70 ± 0.05 eV for all incident energies used.

III. RESULTS

A. Nearly perfect $\text{TiO}_2(110)$

The results of the reflection EELS measurements of the annealed $\text{TiO}_2(110)$ surface for incident electron energies, E_i , of 60 and 1000 eV are presented in Figs. 1(a) and 1(b), respectively. The features labeled *B*, *C*, *D*, *F*, *G*, *H*, *I*, and *J* in Fig. 1(a) and those labeled *E*, *K*, *L*, and *M* in Fig. 1(b) correspond to energy-loss values, E_L , of 5.8, 10.3, 13.5, 23.0, 25.8, 34.8, 37.1, and 38.8 eV, and to 18, 46.5, 51.3, and 62.4 eV, respectively. We have also taken $n(E)$ spectra directly and have obtained features identical to these. For convenience, the loss features have been collected in Table I.

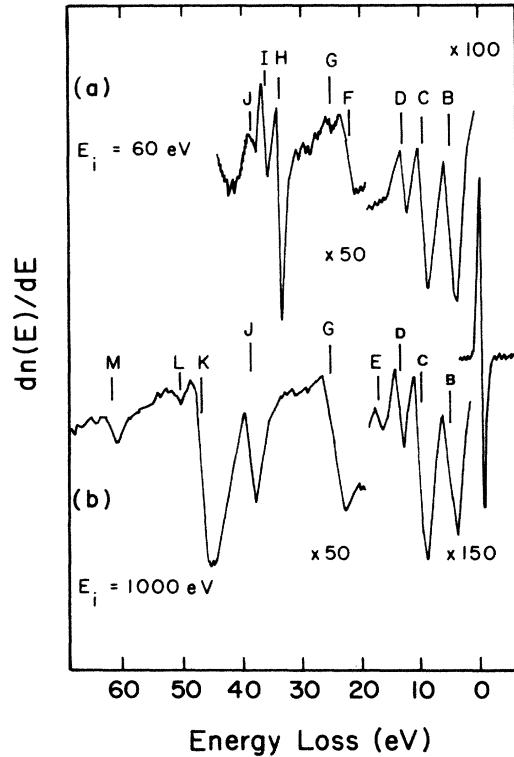


FIG. 1. Electron-energy-loss spectra for the annealed $\text{TiO}_2(110)$ surface taken with incident electron energies, E_i , of (a) 60 eV and (b) 1000 eV.

Figure 2 shows the dependence of the intensities of features *F* through *M* on E_i from 100 to 1000 eV. The intensities of *B*, *C*, and *D* do not depend markedly on E_i and have, therefore, not been included. For $150 \leq E_i \leq 1000$ eV, the intensities have been normalized to that of feature *M*, the intensity of which varies little with E_i . The $E_i = 100$ eV spectrum is normalized to the others by using feature *K*, since its intensity scarcely changes for $E_i \leq 300$ eV.

As can be seen from Fig. 2, the intensities of features *G*, *J*, and *K* increase as E_i is increased from 100 to 1000 eV. The intensities of features *H* and *I* decrease with increasing E_i until they eventually disappear. The intensity of feature *F* also decreases appreciably with increasing E_i : *F* is more dominant than *G* at $E_i \leq 60$ eV [Fig. 1(a)], but *G* appears to become the more dominant at $E_i \geq 500$ eV. The intensities of *L* and *M* increase only slightly with increasing E_i .

B. Effect of Ar^+ -ion bombardment and the evaporation of Ti on $\text{TiO}_2(110)$

Figure 3 presents the EELS spectra for a $\text{TiO}_2(110)$ surface damaged by Ar^+ -ion bombardment; these spectra were obtained after the surface was bombarded with 0.5-keV Ar^+ ions for the cumulative times indicated on each curve. Steady-state conditions are reached after 12–15 min of sputtering. The most noticeable change in the low-energy region of the loss spectrum is the appearance of a new loss feature labeled *A* at 1.5–1.9 eV. Also, the

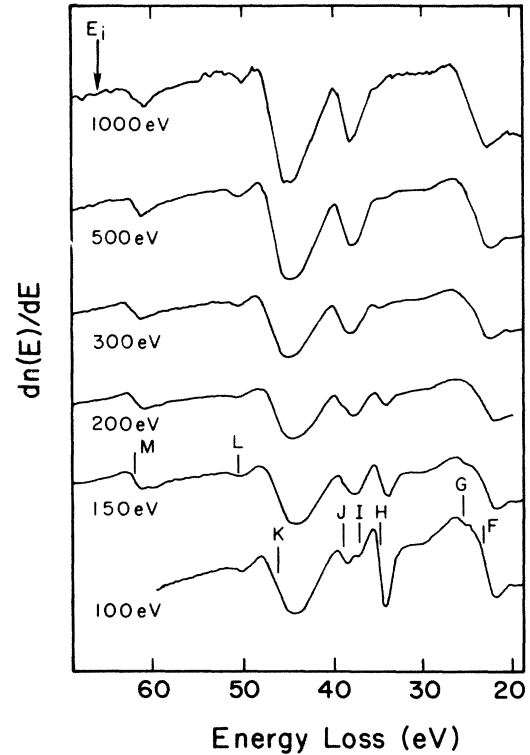


FIG. 2. Electron-energy-loss spectra for annealed $\text{TiO}_2(110)$ showing the dependence of the intensities of the core loss features on primary energy E_i .

relative intensities of features *B*, *C*, and *D* are seen to decrease with increasing density of surface defects, with feature *C* exhibiting the largest effect. In the high-energy-loss region, surface defects have a marked effect on features *I*, *J*, and *L* (not shown here), which disappear after only a small number of defects are created, and on *F*, which is considerably reduced; feature *H* undergoes a noticeable change in shape. Features *J* and *L* can be recovered if incident energies higher than 130 eV are used. The behavior of the various loss features with Ar^+ -ion bombardment is summarized in Table II.

Figure 4 presents core loss spectra obtained from annealed and Ar^+ -ion-bombarded $\text{TiO}_2(110)$ surfaces and from a $\text{TiO}_2(110)$ surface onto which a thin (1.3-Å) layer of Ti was evaporated. It shows that the presence of a thin layer of Ti on $\text{TiO}_2(110)$ causes changes in the core loss spectra which are very similar to those brought about by Ar^+ -ion bombardment. The effect of Ti evaporation on the valence excitation was also obtained and was found identical to that reported previously.¹⁵ As expected, the evaporation of Ti onto $\text{TiO}_2(110)$ results in spectra which are identical to those following Ar^+ -ion bombardment.

IV. COMPARISON WITH OTHER REFLECTION ENERGY-LOSS MEASUREMENTS REPORTED IN THE LITERATURE

The only other reflection electron-energy-loss measurements on TiO_2 which extend to the region spanning the

TABLE I. EELS features for annealed TiO₂ observed at (a) $E_i = 60$ eV and at (b) $E_i = 1000$ eV, and compared with Knotek's results at (a) $E_i = 60$ eV and at (b) $E_i = 200$ eV.

Feature	Present results E_L (eV)	Assignment	Feature (eV)	Knotek's results ^a Assignment
(a) Annealed TiO ₂				
<i>B</i>	5.8	O 2 <i>p</i> (π)-2 <i>t</i> _{2<i>g</i>}	5.5	O 2 <i>p</i> -Ti 3 <i>d</i>
<i>C</i>	10.3	O 2 <i>p</i> (σ)-3 <i>e</i> _{<i>g</i>}	10.3	O 2 <i>p</i> -Ti 3 <i>d</i>
<i>D</i>	13.5	O 2 <i>p</i> (π)-3 <i>a</i> _{1<i>g</i>}	13.5	O 2 <i>p</i> -Ti 3 <i>d</i>
<i>F</i>	23.0	O 2 <i>s</i> -2 <i>t</i> _{2<i>g</i>}	21.8	O 2 <i>s</i> -surface or conduction- band states of oxygen origin
<i>G</i>	25.8	Plasmon excitation		
<i>H</i>	34.8	Ti 3 <i>p</i> -2 <i>t</i> _{2<i>g</i>}	33.6	Ti 3 <i>p</i> -Ti 3 <i>d</i>
<i>I</i>	37.1	Ti 3 <i>p</i> -3 <i>e</i> _{<i>g</i>}	36.0	Ti 3 <i>p</i> -Ti 3 <i>d</i>
<i>J</i>	38.8	O 2 <i>s</i> -4 <i>t</i> _{1<i>u</i>}	38.6	Ti 3 <i>p</i> -Ti 3 <i>d</i>
(b) Annealed TiO ₂				
<i>B</i>	5.8	O 2 <i>p</i> (π)-2 <i>t</i> _{2<i>g</i>}	5.5	O 2 <i>p</i> -Ti 3 <i>d</i>
<i>C</i>	10.3	O 2 <i>p</i> (σ)-3 <i>e</i> _{<i>g</i>}	10.3	O 2 <i>p</i> -Ti 3 <i>d</i>
<i>D</i>	13.5	O 2 <i>p</i> (π)-3 <i>a</i> _{1<i>g</i>}	13.5	O 2 <i>p</i> -Ti 3 <i>d</i>
<i>E</i>	18			
<i>F</i>	23.0	O 2 <i>s</i> -2 <i>t</i> _{2<i>g</i>}	22.6	O 2 <i>s</i> -conduction band
<i>G</i>	25.8	Plasmon excitation		
<i>H</i> and <i>I</i> not seen			33.6	Ti 3 <i>p</i> -Ti 3 <i>d</i>
<i>J</i>	38.8	O 2 <i>s</i> -4 <i>t</i> _{1<i>u</i>}	36.6	Ti 3 <i>p</i> -Ti 3 <i>d</i>
<i>K</i>	46.5	Ti 3 <i>p</i> -Ti 3 <i>d</i> , quasiatomic transition ^b		
<i>L</i>	51.3	O 2 <i>s</i> -4 <i>a</i> _{1<i>g</i>}		
<i>M</i>	62.4	Ti 3 <i>s</i> -2 <i>t</i> _{2<i>g</i>}		

^aReference 10.

^bReference 24.

valence, O 2*s*, and Ti 3*p* excitations have been reported by Knotek¹⁰ for TiO₂(100) using $E_i = 60$ and 200 eV. He also reported the effect of 1-keV Ar⁺-ion bombardment on the EELS results of the annealed surface as well as the dependence of the intensities of the EELS features on E_i . The EELS features obtained by Knotek for $E_i = 60$ and 200 eV are also given in Table I. As can be seen from Table I, the first three features obtained by Knotek for annealed TiO₂ have E_L values nearly identical to those of *B*, *C*, and *D* obtained here and elsewhere.⁷⁻⁹ However, the rest of the EELS features obtained by him do not appear to agree with our features *F* through *J*. We also do not observe any significant shift of the E_L values of the features obtained here with E_i . Nevertheless, it is possible to find a correspondence between the respective loss features on the basis of the dependence of their intensities on the variation of E_i and on the creation of surface defects by Ar⁺-ion bombardment: Thus feature *F* corresponds to Knotek's EELS features at about 22 eV, and our features *H* and *I* to his at $E_L = 33.6$ and 36.0 eV, respectively. The feature seen by Knotek at 38.6 eV for $E_i = 60$ eV could by virtue of its E_L value correspond to our *J*, except that Knotek's is not present in the spectrum for $E_i \geq 200$ eV, where it is replaced by the feature at 36.6

eV. As was stated earlier, the intensity of *J*, on the other hand, becomes larger with increasing E_i . A correspondence between *J* and his feature at 38.6 eV is therefore unlikely. *J* appears to correspond, however, to his feature at 36.6 eV.

The reasons for the difference in the E_L values between our EELS features *F* through *J* and the corresponding features observed by Knotek are not clear. We note, though, that Knotek's measurements were recorded in the second-derivative mode, which could introduce distortions in the features.¹⁶ As was indicated previously, we took data both in the $n(E)$ and $dn(E)/dE$ modes and found them to contain identical features.

The effect of Ar⁺-ion bombardment on Knotek's EELS results is quite similar to the effect observed here. The EELS features obtained by Knotek following 1-keV Ar⁺-ion bombardment are given in Table III. As can be seen from Table III, the valence excitation spectrum has a new loss feature at approximately 2.5 eV and the intensities of the features at 5.5, 10.3, and 13.5 eV are reduced in a manner similar to that of Fig. 3. The core loss spectrum also undergoes a change similar to that seen in Fig. 3: For $E_i = 60$ eV, two features at 25.4 and 33.6 eV are seen in the loss region $30 < E_L < 40$ eV, while for $E_i = 200$

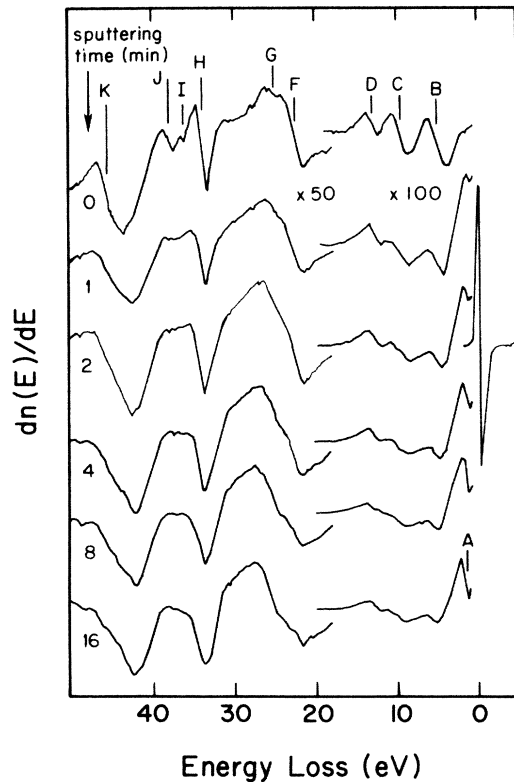


FIG. 3. Electron-energy-loss spectra for $E_i = 100$ eV for Ar^+ -ion bombardment of the annealed $\text{TiO}_2(110)$ surface for the cumulative times indicated.

eV three features at 24.6, 33.6, and 36.6 eV are observed, which again is in qualitative agreement with our results.

The core EELS results for $30 < E_L < 50$ eV of oxidized titanium have also been reported.^{12,13} Ross and Gaugler¹² exposed polycrystalline titanium to 24 L (1 L = 10^{-6} Torr sec) of oxygen, and for $E_i = 200$ eV observed three features at 35, 38.0, and 47 eV, while Roman *et al.*¹³ exposed polycrystalline titanium to 5000 L, and at $E_i = 250$ eV observed two features at 38.5 and 47.0 eV.

TABLE II. EELS features of sputtered TiO_2 obtained here for $E_i = 100$ eV.

Feature	E_L (eV)	Assignment
A	1.9	$2t_{2g} - 2t_{2g}$
B	5.8	$\text{O } 2p(\pi) - 2t_{2g}$
C	10.3	$\text{O } 2p(\sigma) - 3e_g$
D	13.5	$\text{O } 2p(\pi) - 3a_{1g}$
F	Very weak	
G	25.4	Plasmon excitation
H	35.0	$\text{Ti } 3p - 2t_{2g}$
I	Disappeared	
J	Disappeared	
K	45.3	$\text{Ti } 3p - \text{Ti } 3d$ quasiatomic transition
L	Disappeared	

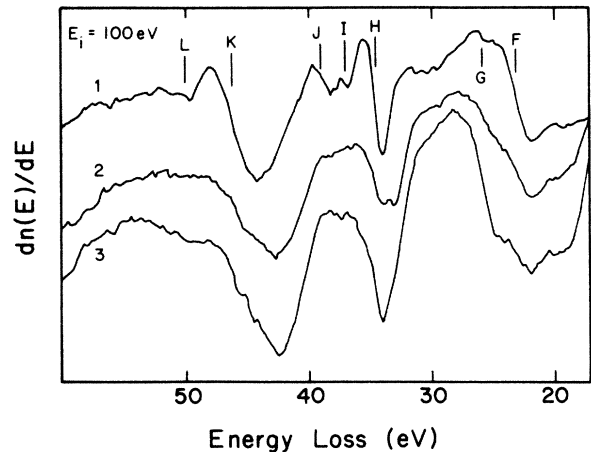


FIG. 4. Electron-energy-loss spectra for $E_i = 100$ eV from annealed $\text{TiO}_2(110)$ (curve 1), from a Ti overlayer on $\text{TiO}_2(110)$ (curve 2) and from Ar^+ -ion bombarded $\text{TiO}_2(110)$ surface (curve 3).

We also have taken extensive core loss measurements on titanium exposed to oxygen exposures of up to 7×10^7 L and have obtained at the respective E_i values features similar to those reported by Ross and Gaugler¹² and by Roman *et al.*¹³ The core loss features obtained for oxidized titanium by Ross and Gaugler and by Roman *et al.* as well as those obtained by us have been collected in Table IV.

V. DISCUSSION OF RESULTS

As is shown in Fig. 2 and as was indicated by Knotek,¹⁰ the intensities of features *F*, *H*, and *I* are found to decrease dramatically with increasing E_i . This might suggest, as Knotek indicated, the presence of either intrinsic surface states or excitonic effects. However, it is now well established that there are no surface states in the case of defect-free TiO_2 . Results of several types of theoretical studies on perfect surfaces⁴ as well as experimental measurements on three different vacuum-cleaved TiO_2 (Ref. 17) faces have now been reported which conclude that, at least for $\text{TiO}_2(110)$, there are no identifiable surface states whose electronic structure differs from that of bulk TiO_2 . Also, the dramatic reduction in the intensities of *F* and *H* as E_i is increased from 100 to 150 eV and in that of feature *I* as E_i is increased from 60 to 100 eV discounts arguments based on the variations with E_i of the escape depth of inelastically scattered electrons, since the escape depth is not expected to change appreciably over such a short energy interval. Excitonic effects can likewise be discounted since similar reductions in the intensities of the Ti $3p$ excitations with increasing E_i have been observed in the EELS spectra of both Ti and Ti_2O_3 ,¹⁸ and since an interpretation based on single-electron inelastic scattering can be advanced here. Since intrinsic surface states and excitonic effects are unlikely, we attribute the intensity changes to cross-sectional effects.

TABLE III. EELS features of sputtered TiO₂ obtained by Knotek (Ref. 10).

$E_i = 60$ eV		$E_i = 200$ eV	
Feature (eV)	Assignment	Feature (eV)	Assignment
2.5	(Ti 3 <i>d</i> – Ti 3 <i>d</i>)	2.5	(Ti 3 <i>d</i> – Ti 3 <i>d</i>)
5.5	O 2 <i>p</i> – Ti 3 <i>d</i>	5.5	O 2 <i>p</i> – Ti 3 <i>d</i>
10.3	O 2 <i>p</i> – Ti 3 <i>d</i>	10.3	O 2 <i>p</i> – Ti 3 <i>d</i>
13.5	O 2 <i>p</i> – Ti 3 <i>d</i>	13.5	O 2 <i>p</i> – Ti 3 <i>d</i>
25.4 instead of 21.8	O 2 <i>s</i> – conduction- band states	24.6 instead of 22.6	O 2 <i>s</i> – conduction- band states
33.6	Ti 3 <i>p</i> – Ti 3 <i>d</i>	33.6 as a shoulder	
36.0	Disappeared	36.6	Ti 3 <i>p</i> – Ti 3 <i>d</i>
38.6	Disappeared		

The effect of Ar⁺-ion bombardment on the TiO₂(110) surface has been studied by several groups using UPS and EELS.^{4–6} These techniques have indicated the presence of occupied states in the bulk band gap as a result of the preferential loss of lattice oxygen ions from the surface; these gap states are not detected in a defect-free sample. In the published EELS results these newly introduced occupied states manifest themselves by the appearance in the EELS spectrum of the feature labeled *A* in Fig. 3, which has been attributed to a transition between the occupied and the unoccupied Ti 3*d* orbitals.¹⁴ The changes occurring in the core loss region following Ar⁺-ion bombardment are similarly the consequence of the loss of lattice oxygen ions.

As was mentioned earlier, the evaporation of Ti on TiO₂ causes changes in the core loss spectra which are identical to those produced by Ar⁺-ion bombardment.¹² Although lattice oxygen ions are not being removed as in

the case of Ar⁺-ion bombardment, the presence of the additional Ti overlayer changes the oxygen-titanium ratio at the surface to give a final state similar to that caused by Ar⁺-ion bombardment.

Figure 5 presents a schematic diagram of the unoccupied symmetry-based molecular-orbital (MO) energy levels which were empirically deduced from x-ray-absorption spectroscopy (XAS) measurements of the *K* edges of O and Ti in TiO₂.^{19–21} Also shown are the transitions between the initially-filled levels of O 2*s*, Ti 3*p*, and Ti 3*s* and these empty MO levels. Molecular orbital theory has been found adequate to explain the Ti *K* and O *K* XAS results for TiO₂ and will be used here also. Our assignment of the features *F*, *H*, *I*, *J*, *L*, and *M* have also been indicated in Table I. Unlike that of *J*, the intensities of features *L* and *M* show a very weak dependence on E_i . Feature *M* has previously been attributed to a quadrupole-allowed Ti 3*s* – Ti 3*d* transition for both Ti

TABLE IV. EELS features of oxidized titanium in the loss region $30 < E_L < 40$ eV.

Incident energy E_i (eV)	Work	Oxygen exposure (L)	Feature (eV)	Assignment
100	Present work	30 and 72×10^6	35 (<i>H</i>)	Ti 3 <i>p</i> – 2 <i>t</i> _{2<i>g</i>}
			38.8 (<i>J</i>)	O 2 <i>s</i> – 4 <i>t</i> _{1<i>u</i>}
			47 (<i>K</i>)	Ti 3 <i>p</i> – Ti 3 <i>d</i> , quasiatomic transition
200	Ross and Gaugler ^a	24	35.0	Due to Ti 3 <i>p</i> excitation in TiO oxide phase
			38.0	Due to Ti 3 <i>p</i> excitation in TiO ₂ oxide phase
			47.0	Not discussed
250	Roman <i>et al.</i> ^b	5000	38.5	Due to Ti 3 <i>p</i> excitation in a TiO ₂ oxide phase
			47	Ti 3 <i>p</i> – Ti 3 <i>d</i>

^aReference 12.^bReference 13.

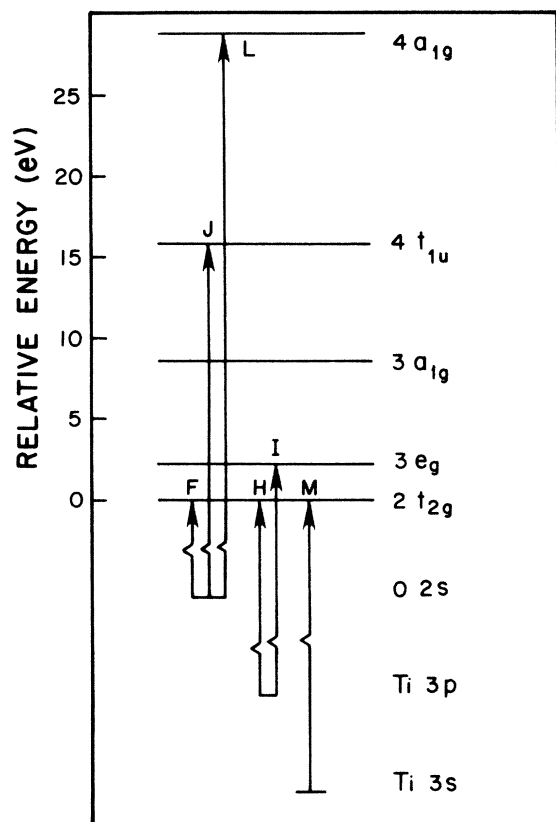


FIG. 5. Schematic molecular-orbital energy diagram for TiO_2 showing assignment of the EELS features.

and oxygen-exposed Ti.²² Because of the similarities of L and M we believe that L also represents a quadrupole-allowed transition, as shown in Fig. 5. The loss features B , C , and D of Fig. 1 and feature A of Fig. 3 have been interpreted previously and will not be considered further. Feature E is not always present in the spectra, and when it is present it occurs only for $E_i > 250$ eV; further study is required before more can be said about this feature. Feature G has been attributed to the collective excitation of the valence electrons²³ and K , which is seen in the spectra of both the metal and its oxides, has been discussed in recent publications and has been attributed to a localized quasiatomic transition between the Ti $3p$ and Ti $3d$ orbitals.^{18,24}

Our assignment of J differs from that suggested by Knotek,¹⁰ shown in Table I(a), and by Roman *et al.*¹³ (see Table IV), while both this assignment and that given to H are contrary to those suggested by Ross and Gaugler (see Table IV).¹² The interpretations proposed for J by Knotek¹⁰ and by Roman *et al.*¹³ and for H and J by Ross and Gaugler¹² have been influenced by the apparent agreement between the binding energies of the Ti $3p$ core level in TiO_2 and TiO as found from XPS and the E_L values of J and H , respectively, and by the assumption by Ross and Gaugler that distinct oxides, here TiO and TiO_2 , can coexist for oxygen exposures of 24 L. The interpretation proposed for H ($E_L = 35$ eV) by Ross and

Gaugler is not convincing. Were their interpretation to be correct, the 35-eV feature should have shifted in energy and should have eventually disappeared from the spectrum with increasing oxygen exposures. This does not happen, which is not surprising as H is observed also for defect-free TiO_2 .

The association of J ($c \sim 38$ eV) with an excitation originating from the Ti $3p$ core level in TiO_2 is also not correct. The apparent agreement between the E_L value of J and the binding energy of the Ti $3p$ core level (~ 38 eV) of TiO_2 , as obtained from x-ray photoemission spectroscopy^{25,26} (XPS) is accidental. Firstly, the chemical shifts derived from XPS and EELS need not be the same. The XPS-derived chemical shifts (oxide binding energy–metal binding energy) are of the order of 5 eV for all Ti core orbitals in TiO_2 , whereas the chemical shifts obtained from EELS measurements are smaller and not even the same for different Ti core levels: These are approximately 1.5 eV for the $2p$ level but 4 eV for the $3s$ level.^{27,22} We also have observed a shift of approximately 2 eV for the $3p$ level during oxidation of Ti. Also, threshold spectroscopies such as soft-x-ray appearance-potential²⁸ and Auger electron appearance-potential spectroscopy²⁹ show chemical shifts for the Ti $2p$ level of 2 and 1.5 eV, respectively. It therefore appears that one should be careful in using chemical shifts derived by different techniques. At any rate, the first core loss feature occurring at $E_L > 33$ eV (33 eV being the E_L value corresponding to the excitation of the Ti $3p$ level in the metal) following oxidation of titanium is H ($E_L \approx 35$ eV) and not J ($E_L \approx 39$ eV). The reason Roman *et al.*¹³ did not observe H after oxidizing titanium is partly because they used high primary energy ($E_i = 250$ eV) and partly because of their poor energy resolution (≈ 2 eV from the FWHM of their elastic peak). As was shown in Fig. 2, the intensity of feature H is a strong function of the energy of the incident electrons. Secondly, as was discussed before, Ar^+ -ion bombardment of TiO_2 as well as the evaporation of Ti on the surface cause feature J to disappear from the spectrum in surface-sensitive measurements along with that of L , while causing only some broadening of the feature H and some slight shift in the E_L values of K and M . The core loss features F , H , J , K , L , and M can therefore be put into two groups according to whether or not their intensities are markedly diminished when the TiO_2 surface is reduced. Thus, features H , K , and M fall into one group while features F , J , and L fall into another. The features in the former group have been attributed to transitions originating from Ti core levels (H and K from Ti $3p$, and M from Ti $3s$), and it is not surprising to find these transitions still present in the EELS spectra. The marked reduction in the intensity of feature F and the disappearance of J and L are also to be expected as the O-Ti ratio at the surface is drastically reduced by either Ar^+ -ion bombardment or by a Ti overlayer; this behavior is compatible with the assignment shown in Fig. 5. Attributing J to transitions involving the oxygen core level is thus manifestly more consistent with the effects of surface defects than is its assignment to a transition originating from Ti $3p$ core level, as has been

done previously.^{10,12,13.}

Before suggesting the reasons underlying the disappearance of feature *I* and the broadening of feature *H* following sputtering and Ti evaporation, we recall that, for TiO₂, band-structure calculations³⁰ as well as XAS (Refs. 19 and 21) and transmission EELS measurements¹⁹ indicate that the *2t_{2g}* and *3e_g* orbitals (both mainly Ti *3d* states) are resolved and are separated by 2–3 eV. In contradistinction, the conduction-band density of states of TiO_x ($0.8 \leq x \leq 1.22$) shows, according to band-structure calculations,³¹ a single broad peak. In agreement with this, the Ti *3p* near-threshold EELS spectra of Ti₂O₃ show a single broad (FWHM of ≈ 5.0 eV) loss feature.¹⁸ Since the TiO₂ surface is thought to be reduced to lower Ti oxides both by Ar⁺-ion bombardment and by a Ti evaporation, it is reasonable and consistent with the above that the Ti *3p* near-threshold EELS features *H* and *I* of TiO₂ be replaced by a single broad feature *H* following a reduction of the surface. We therefore believe that the disappearance of feature *I* accompanied by a broadening of *H* is due to the changes in the profile of the conduction-band density of states associated with the reduction of the TiO₂ surface.

VI. SUMMARY

We have measured the electron-energy-loss spectra of the defect-free TiO₂(110) surface which include excita-

tions of the O *2s*, Ti *3p*, and Ti *3s* core levels, and we have investigated the effect Ar⁺-ion bombardment and the evaporation of Ti have on the EELS features of annealed TiO₂. Also investigated was the dependence of the intensities of the observed loss features on incident electron energy *E_i*.

The results have been interpreted using the unoccupied molecular-orbital energy levels derived from XAS, bearing in mind the observed dependence of the loss features on the reduction of the oxide surface. The loss feature at 38.8 eV for TiO₂ has been reinterpreted, as have the loss features at 35 and 38.5 previously reported for oxidized titanium.

Finally, we have demonstrated that the core loss results of TiO₂ are extremely sensitive to the presence of surface defects because these defects change the surface stoichiometry. This sensitivity can then be used to discriminate between core loss features arising from different components of the transition metal compound.

ACKNOWLEDGMENTS

This work was partially supported by the National Science Foundation, Solid State Chemistry Program Grant No. DMR-82-02727.

*Present address: Department of Physics, Indiana University, Bloomington, IN 47405.

†Present address: Sachs/Freeman Associates, Inc., Landover, MD 20785.

¹A. Fujishima and K. Honda, *Nature* **238**, 37 (1972).

²S. J. Tauster, S. C. Fung, and R. L. Garten, *J. Am. Chem. Soc.* **100**, 170 (1978).

³H. R. Sadeghi and V. E. Henrich, *Appl. Surf. Sci.* **19**, 330 (1984).

⁴V. E. Henrich, *Rep. Prog. Phys.* **48**, 1481 (1985).

⁵V. E. Henrich, *Prog. Surf. Sci.* **14**, 175 (1983).

⁶V. E. Henrich, *Prog. Surf. Sci.* **9**, 143 (1979).

⁷V. E. Henrich, H. J. Zeiger and G. Dresselhaus, in *Electrocatalysis on Non-Metallic Surfaces*, Natl. Bur. Stand. (U.S.) Special Publ. No. 445 (U.S. GPO, Washington, D. C., 1976).

⁸Y. W. Chung, W. J. Lo and G. A. Somorjai, *Surf. Sci.* **64**, 588 (1977).

⁹W. Gopel, J. A. Anderson, D. Frankel, M. Jaehnig, K. Phillips, J. A. Schafer, and G. Rocker, *Surf. Sci.* **139**, 333 (1984).

¹⁰M. L. Knotek, in *Proceedings of the Symposium on Electrode Materials and Processes for Energy Conversion and Storage*, edited by J. D. E. McIntyre *et al.* (Electrochemical Society, Princeton, 1977), pp. 234–246.

¹¹D. M. Hanson, R. Stockbauer, and T. E. Madey, *Phys. Rev. B* **24**, 5513 (1981).

¹²P. N. Ross, Jr., and K. A. Gaugler, *Surf. Sci.* **122**, L579 (1982).

¹³E. Roman, M. Sanchez-Avedillo, and J. L. de Segovia, *Appl. Phys. A* **35**, 35 (1984).

¹⁴V. E. Henrich, G. Dresselhaus, and H. J. Zeiger, *Phys. Rev. Lett.* **36**, 1335 (1976).

¹⁵W. J. Lo, Y. W. Chung, and G. A. Somorjai, *Surf. Sci.* **71**, 199

(1978).

¹⁶V. E. Henrich, *Appl. Surf. Sci.* **6**, 87 (1980).

¹⁷Victor E. Henrich and Richard L. Kurtz, *Phys. Rev. B* **23**, 6280 (1981).

¹⁸J. M. McKay, M. H. Mohamed, and V. E. Henrich, *Phys. Rev. B* **35**, 4304 (1987).

¹⁹L. A. Grunes, *Phys. Rev. B* **27**, 2111 (1983).

²⁰D. W. Fischer, *Phys. Rev. B* **5**, 4219 (1972).

²¹K. Tsutsumi, O. Aita, and K. Ichikawa, *Phys. Rev. B* **15**, 4638 (1977).

²²L. A. Grunes and R. D. Leapman, *Phys. Rev. B* **22**, 3778 (1980).

²³J. Frandon, B. Brousseau, and F. Pradal, *J. Phys. (Paris)* **39**, 839 (1978).

²⁴E. Bertel, R. Stockbauer, and T. E. Madey, *Surf. Sci.* **141**, 355 (1984).

²⁵S. P. Kowalczyk, F. R. McFeely, L. Ley, V. T. Gritsyna, and D. A. Shirley, *Solid State Commun.* **23**, 161 (1977). Adding the binding energy of the O *2s* core level below the valence-band maximum obtained from this work (19.5 eV) to the gap energy (3.05 eV) we get the binding energy of the O *2s* level below the conduction-band minimum as $19.5 + 3.05 = 22.55$ eV.

²⁶C. N. R. Rao, D. D. Sarma, S. Vasudevan, and M. S. Hegde, *Proc. R. Soc. London, Ser. A* **367**, 239 (1979).

²⁷R. D. Leapman, L. A. Grunes, and P. L. Fejes, *Phys. Rev. B* **26**, 614 (1982).

²⁸R. Konishi and S. Kato, *Jpn. J. Appl. Phys.* **15**, 1237 (1976).

²⁹R. Konishi and S. Kato, *Jpn. J. Appl. Phys.* **23**, 975 (1984).

³⁰S. Munnix and M. Schmeits, *Phys. Rev. B* **30**, 2202 (1984).

³¹J. M. Schoen and S. P. Denker, *Phys. Rev.* **184**, 864 (1969).